

## Hall effect above $T_c$ in untwinned single-crystal $\text{YBa}_2\text{Cu}_3\text{O}_{7-x}$ : Normal-state behavior and superconducting fluctuations

J. P. Rice, J. Giapintzakis, D. M. Ginsberg, and J. M. Mochel

*Department of Physics and Materials Research Laboratory, University of Illinois at Urbana-Champaign,  
1110 West Green Street, Urbana, Illinois 61801*

(Received 10 June 1991; revised manuscript received 21 August 1991)

We present a measurement of the Hall coefficient  $R_H$  for an untwinned single crystal of  $\text{YBa}_2\text{Cu}_3\text{O}_{7-x}$ . The crystal was produced by a method that does not involve thermomechanical detwinning, and has a resistivity along the copper-oxide chains of only  $29 \mu\Omega \text{ cm}$  at 100 K, indicating high sample quality. The in-plane resistivity and  $1/R_H$  become linear in temperature as  $T$  rises significantly above  $T_c$ . Near  $T_c$  we observe deviation from this linearity, and we interpret it as indicating thermodynamic fluctuations in a layered superconductor. Fits of this model to both the resistivity and Hall-effect data yield physically reasonable values for the fitting parameters. Evidence is obtained that the two copper-oxide planes in each unit cell are tightly coupled, acting as one superconducting layer. Surprisingly, the best fits indicate that the Hall-effect fluctuations are dominated by the Maki-Thompson process rather than the Aslamazov-Larkin process.

### I. INTRODUCTION

Effects of superconducting fluctuations have been seen in various properties of high- $T_c$  superconductors, including electrical conductivity,<sup>1,2</sup> specific heat,<sup>3</sup> magnetic susceptibility,<sup>4</sup> magnetoresistance,<sup>5</sup> and Hall effect.<sup>6</sup> In the case of the Hall data, the fluctuation effect in  $\text{YBa}_2\text{Cu}_3\text{O}_{7-x}$  above  $T_c$  is a prominent deviation from the  $1/T$  normal-state dependence of the Hall coefficient  $R_H$  for a magnetic field  $H$  perpendicular to the copper-oxide planes.

Theoretical models for fluctuation effects often involve several parameters, making it difficult to test the theories, since very good fits of the same data to several different models can be obtained if enough parameters are adjusted. In this paper we attempt to reduce the impact of this difficulty by simultaneously measuring two independent quantities, the electrical and Hall conductivities, and comparing them both to the predictions of the same model using the same parameters. Sample quality and homogeneity are of paramount importance in the investigation of fluctuation effects, and so we have performed the experiment on one of the cleanest available high- $T_c$  samples: a thin untwinned single crystal produced by a method not requiring applied stress. Crystals produced by this method have given clean results in several other experiments, including specific heat,<sup>3</sup> Raman effect,<sup>7</sup> torsional oscillator experiments,<sup>8</sup> and conductivity.<sup>9</sup>

### II. CRYSTAL PREPARATION

The untwinned  $\text{YBa}_2\text{Cu}_3\text{O}_{7-x}$  crystal investigated in this study was produced by a method described elsewhere.<sup>10</sup> It was cleaved from a parent crystal into a bar shape suitable for Hall-effect measurements,<sup>11</sup> with dimensions  $190 \times 820 \times 12 \mu\text{m}^3$  along the  $a$ ,  $b$ , and  $c$  axes, respectively. The copper-oxide planes of  $\text{YBa}_2\text{Cu}_3\text{O}_{7-x}$  lie in the  $a$ - $b$  plane, and the copper-oxide chains run

along the  $b$  axis. The current flowed in the  $b$  direction. We choose  $(a, b, c)$  to be a left-handed coordinate system, so the conductivity matrix element  $\sigma_{ab}$  is positive for hole conduction.

A five-probe contact arrangement was used. Two current contacts were made by evaporating gold onto both of the  $190 \times 12 \mu\text{m}^2$   $a$ - $c$  edges. Three voltage contacts  $20 \times 12 \mu\text{m}^2$  in size were made by evaporating gold onto the  $b$ - $c$  edges through a thin slit placed against the crystal. Two of these contacts were on one  $b$ - $c$  edge, and the third was on the opposite  $b$ - $c$  edge. Thus the uniformity of the current density in the planes is essentially undisturbed. We used the two voltage contacts on the same edge to determine a voltage drop along the current direction. We refer to this as the longitudinal voltage. For Hall-effect measurements, a high-resistance potentiometer was connected across the two contacts on the common edge, and we measured the voltage between the wiper of the potentiometer and the third contact. We refer to this as the transverse voltage. It was nulled by adjusting the potentiometer at zero field.

In order to decrease the contact resistance and help the contacts stick, the crystal with its gold contacts was annealed at  $400^\circ\text{C}$  for 48 h in flowing  $\text{O}_2$ . The contact resistance after this procedure was less than  $1 \Omega$ . The crystal remained untwinned during this procedure. A secondary-ion-mass spectroscopy (SIMS) depth profile performed on a similarly prepared twinned crystal demonstrated that the depth of gold diffusion after such a heat treatment was less than  $0.2 \mu\text{m}$  along the  $c$  axis.<sup>9</sup> Thus the effects of contacts are expected to be insignificant.

After annealing the contacts, the crystal was mounted on a single-crystal MgO substrate, onto which a five-wire gold pattern had been evaporated. Silver paste (Du Pont conductor composition 4929N) was used to make electrical contact between the gold contact pads on the crystal and the gold pattern on the substrate. These silver paste connections also anchored the crystal to the substrate.

Since the coefficient of thermal expansion of MgO is similar to that of  $\text{YBa}_2\text{Cu}_3\text{O}_{7-x}$ , differential thermal contraction was minimized. Using GE 7031 varnish, the MgO substrate was then mounted on a copper plate on the bottom of a cryogenic insert.

### III. MEASUREMENTS

A calibrated platinum resistance thermometer was mounted on the copper plate holding the substrate, and data were taken only after achieving thermal equilibrium. The measurements were carried out with the sample in a superconducting magnet, and the field was determined by measuring the current through the (previously calibrated) magnet. The magnetic field  $H$  was applied along the  $c$  axis of the crystal, perpendicular to the copper-oxide planes of  $\text{YBa}_2\text{Cu}_3\text{O}_{7-x}$ .

Computer-controlled instrumentation was used throughout the experiment. A constant-amplitude ac current of 10 mA rms at 37.8 Hz was supplied to the sample from the reference channel of a lock-in amplifier. The rms current density was 440 A/cm<sup>2</sup>. The in-phase longitudinal and transverse voltages were measured with lock-in amplifiers. Current-voltage measurements up to 10 mA rms showed ohmic behavior throughout the temperature region reported here.

In an initial temperature sweep at zero field, the resistivity showed a well-defined superconducting transition with an onset at 94.9 K, midpoint at 94.5 K, zero resistivity (to within the noise level) at 93 K, and a 10–90% transition width of 0.2 K.

We used magnetic-field sweeps at fixed temperatures. The temperature was stable to within 15 mK during each field sweep. Measurements of the longitudinal and transverse resistivities were made over a temperature range from 82 to 280 K and in fields from 0 to 7 T. At each field the longitudinal and transverse resistivities were measured, one immediately after the other.

### IV. RESULTS

In this paper we concentrate on the data above  $T_c$ . The temperature dependence of  $\rho_{bb}$ , the longitudinal resistivity along the  $b$  axis, is shown in Fig. 1. These data were taken at 1 T; data taken at other fields ranging from 0 to 7 T lie on top of these data points, since the magnetoresistance of  $\text{YBa}_2\text{Cu}_3\text{O}_{7-x}$  is small above  $T_c$ . The resistivity was 29  $\mu\Omega\text{cm}$  at 100 K and 96  $\mu\Omega\text{cm}$  at 300 K. These are among the lowest values of resistivity reported so far for  $\text{YBa}_2\text{Cu}_3\text{O}_{7-x}$  and attest to the high quality of the sample.

The contact arrangement that we used did not allow us to measure  $\rho_{aa}$ , the resistivity along the  $a$  axis, on this particular sample. However, in other  $\text{YBa}_2\text{Cu}_3\text{O}_{7-x}$  crystals, produced by us with the same method, the temperature-dependent ratio  $\rho_{aa}/\rho_{bb}$  has been measured and found to be reproducible.<sup>9</sup> Using this temperature-dependent anisotropy ratio, we calculated the  $\rho_{aa}$  data shown in Fig. 1 from our  $\rho_{bb}$  data. That there is a factor of about 2.2 between the  $a$  and  $b$  resistivities indicates the importance of using untwinned crystals for measurements

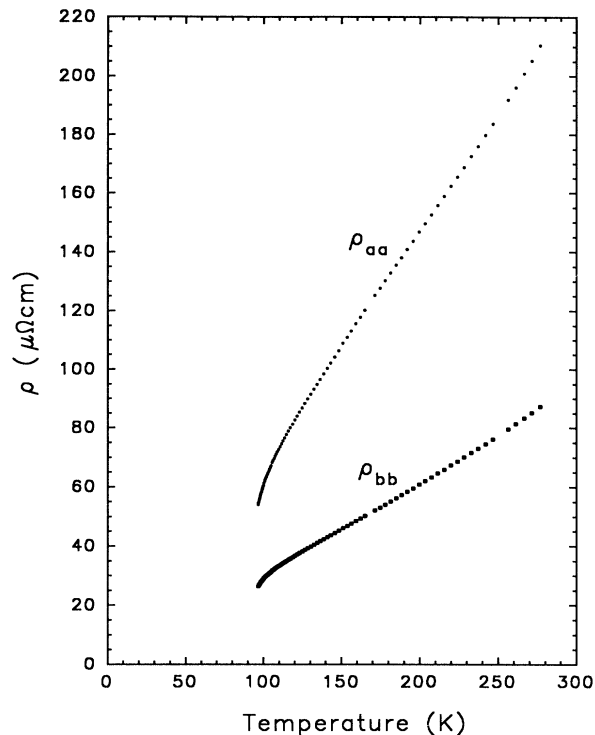


FIG. 1.  $a$  and  $b$  resistivities of the crystal as a function of temperature. The data were taken with a field of 1 T applied along the  $c$  axis.

of resistivity and Hall effect in  $\text{YBa}_2\text{Cu}_3\text{O}_{7-x}$ .

The apparent transverse resistivity  $\rho_{\text{tran}}$  had a linear field dependence up to 7 T for all temperatures greater than 96.70 K. At lower temperatures,  $\rho_{\text{tran}}$  took on a nonlinear field dependence, which we do not present or discuss in this paper. The slope of each  $\rho_{\text{tran}}$ -vs- $H$  curve gives the Hall coefficient  $R_H$ . We concentrate only on the data above 96.70 K, where the Hall coefficient is independent of field. Zero-field values of  $\rho_{\text{tran}}$  reflect a small component of contact misalignment voltage that was not precisely nulled by the potentiometer, and are not physically significant. At each temperature these zero-field values were subtracted from the in-field values of  $\rho_{\text{tran}}$  to yield values of the Hall resistivity,  $-\rho_{ab}$ , shown in Fig. 2 for Hall field along  $a$ , current density along  $b$ , and magnetic field along  $c$ . In Fig. 3  $-\rho_{ab}$  is shown for each field as a function of temperature. In the inset of Fig. 4 we plot the temperature dependence of the reciprocal of the Hall coefficient, scaled to indicate carriers per unit cell. In agreement with other authors,<sup>6,12,13</sup> working with twinned samples, we find that the carriers in the  $a$ - $b$  plane are holes and that their density increases from about 0.8 carriers per unit cell near 100 K to about 2 carriers per unit cell at room temperature. We caution that this carrier density determined from Hall-effect measurements is not necessarily the true carrier density of the material, because of the use of the one-band model. The

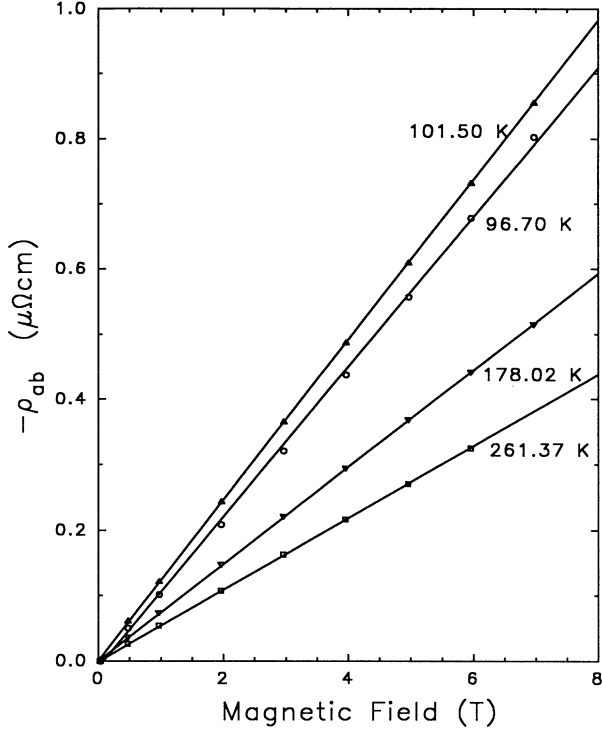


FIG. 2. Hall resistivity as a function of field at various representative temperatures, showing linear behavior.

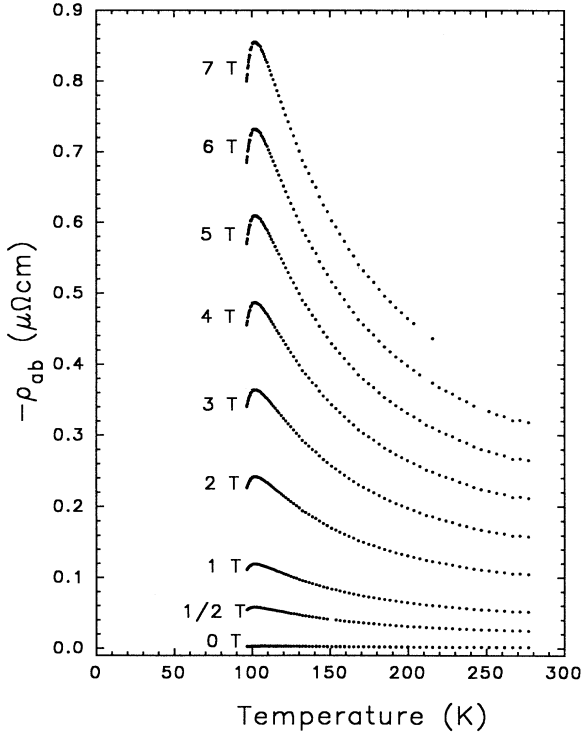


FIG. 3. Hall resistivity as a function of temperature at various fields, showing the  $1/T$  dependence in the normal state and the dramatic rounding just above  $T_c$  resulting from superconducting fluctuations.

upturn just above  $T_c$  will be interpreted as showing superconducting fluctuations.

## V. ANALYSIS

We have measured elements of the resistivity tensor:  $\rho_{aa}$  and  $\rho_{bb}$  are the diagonal resistivities, while the off-diagonal elements  $\rho_{ab}$  and  $\rho_{ba}$  represent the Hall resistivity and are related to each other through the Onsager relation<sup>14</sup>

$$\rho_{ab}(\mathbf{H}) = \rho_{ba}(-\mathbf{H}). \quad (1)$$

For comparison with theoretical expressions, we invert the resistivity tensor to obtain the elements of the conductivity tensor. The Hall conductivity  $\sigma_{ab}$  is given by

$$\sigma_{ab} = \frac{-\rho_{ab}}{\rho_{aa}\rho_{bb} - \rho_{ab}\rho_{ba}} \approx R_H H \sigma_{aa} \sigma_{bb}. \quad (2)$$

Since the maximum Hall angle measured in this experiment is less than  $2^\circ$ , the approximation of neglecting the product  $\rho_{ab}\rho_{ba}$  in the denominator is good to within 1 part in 1000. For the same reason,  $\sigma_{aa}$  and  $\sigma_{bb}$  are almost exactly the reciprocals of  $\rho_{aa}$  and  $\rho_{bb}$ , respectively.

We interpret the data in terms of a model of superconducting fluctuations above  $T_c$  in a layered superconductor.<sup>15,16</sup> This model assumes that the crystal is made up of layers of superconducting planes, presumably the copper-oxide planes in  $\text{YBa}_2\text{Cu}_3\text{O}_{7-x}$ , spaced by a uniform distance which we denote as  $s$ . The model ignores the copper-oxide chains and assumes that the superconducting planes are isotropic. However, the in-plane conductivity is anisotropic in  $\text{YBa}_2\text{Cu}_3\text{O}_{7-x}$ .<sup>9</sup> For comparison to the model we therefore use an isotropic mean conductivity  $\sigma_{mm}$ , defined by

$$\sigma_{mm} = \frac{1}{2}(\sigma_{aa} + \sigma_{bb}). \quad (3)$$

Thus two independent quantities  $\sigma_{mm}$  and  $\sigma_{ab}$  are compared with theory as a function of temperature.

Above  $T_c$  there are normal-state and fluctuation contributions to the conductivity, denoted by  $\sigma_{mm}^0$  and  $\Delta\sigma_{mm}$ , respectively:

$$\sigma_{mm} = \sigma_{mm}^0 + \Delta\sigma_{mm}. \quad (4)$$

Similarly, for the Hall conductivity,

$$\sigma_{ab} = \sigma_{ab}^0 + \Delta\sigma_{ab}. \quad (5)$$

The resistivity is very linear in temperature over a range from 120 to 180 K (Fig. 1). The reciprocal of the Hall coefficient is also linear in temperature over this range and actually has a zero intercept (Fig. 4). We assume that these forms hold for the normal-state contribution to the resistivity and Hall coefficient over the entire temperature range from 95 to 180 K:

$$\sigma_{mm}^0 = \frac{1}{aT + b}, \quad (6)$$

$$R_H^0 = \frac{1}{cT}, \quad (7)$$

where  $a$ ,  $b$ , and  $c$  are constants. We determine  $c$  by fitting Eq. (7) to the  $R_H$  data over a temperature range from 141 to 178 K. We find  $c = 7.624 \times 10^4$  T/( $\Omega$  cm K). This is an excellent fit, as is shown in Fig. 4. The normal-state Hall conductivity is then expressed in a way consistent with Eqs. (2)–(7) by

$$\sigma_{ab}^0 = \frac{4\gamma}{(1+\gamma)^2} R_H^0 H (\sigma_{mm}^0)^2, \quad (8)$$

where  $\gamma$  is the temperature-dependent  $a$ - $b$  resistivity anisotropy ratio measured by Friedmann *et al.*:<sup>9</sup>

$$\gamma = \frac{\rho_{aa}}{\rho_{bb}} \approx \frac{\sigma_{bb}}{\sigma_{aa}}. \quad (9)$$

We consider two contributions to the fluctuation conductivity above  $T_c$ , the Aslamazov-Larkin<sup>17</sup> (AL) term and the Maki-Thompson<sup>18</sup> (MT) term. The AL contribution results directly from the superconducting fluctuations, whereas the MT contribution results from the interaction of normal excitations with the superconducting fluctuations. In the three-dimensional (3D) and two-dimensional (2D) limits, these are

$$\Delta\sigma_{mm}^{(3D)} = \frac{e^2}{32\hbar\xi_c(0)} (4\eta^{-1/2} + \eta^{-1/2}), \quad (10a)$$

$$\Delta\sigma_{mm}^{(2D)} = \frac{e^2}{16\hbar s} \left[ \frac{2}{\eta - \delta} \ln \left[ \frac{\eta}{\delta} \right] + \eta^{-1} \right]. \quad (10b)$$

Here  $\eta$  is the reduced temperature defined by

$$\eta = \ln \left[ \frac{T}{T_c} \right] \approx \frac{T - T_c}{T_c}. \quad (11)$$

$\xi_c(0)$  is the zero-temperature value of the Ginzburg-Landau coherence length,  $s$  is the film thickness (which becomes the layer spacing in the layered-structure model), and  $\delta$  is the Maki-Thompson pair-breaking parameter. The first term in the square brackets in Eqs. (10a) and (10b) is the MT term; the second is the AL term. Fukuyama, Ebisawa, and Tsuzuki<sup>19</sup> studied the effect of the AL and MT processes on the Hall conductivity and derived the 3D and 2D forms:<sup>20</sup>

$$\Delta\sigma_{ab}^{(3D)} = \frac{e^2}{16\hbar\xi_c(0)} \frac{\sigma_{ab}^0}{\sigma_{mm}^0} \left[ 4\eta^{-1/2} + \frac{7\pi\alpha}{36}\eta^{-3/2} \right], \quad (12a)$$

$$\Delta\sigma_{ab}^{(2D)} = \frac{e^2}{8\hbar s} \frac{\sigma_{ab}^0}{\sigma_{mm}^0} \left[ \frac{2}{\eta - \delta} \ln \left[ \frac{\eta}{\delta} \right] + \frac{\pi\alpha}{36}\eta^{-2} \right], \quad (12b)$$

where  $\alpha$  is a dimensionless parameter which depends upon the microscopic details. Again, the first term in the square brackets is the MT term, and the second is the AL contribution. Since  $\alpha$  can, in general, be positive or negative,<sup>19</sup> the fluctuation Hall conductivity can be positive or negative.

The temperature-dependent Ginzburg-Landau coherence length is expected to increase from its zero-temperature value as  $T_c$  is approached from above or below. Far above  $T_c$ , where  $\xi_c(T)$  is small compared to the layer spacing  $s$ , the superconducting layers are decoupled, and 2D behavior is approached. Just above  $T_c$ , where  $\xi_c(T)$  becomes larger than  $s$ , the layers become coupled, and 3D behavior is approached. To quantify these two limits, we define a dimensionless parameter  $d$  by

$$d = \frac{s}{2\xi_c(0)}. \quad (13)$$

The 2D limit is when  $d^2\eta \gg 1$ , and the 3D limit is when  $d^2\eta \ll 1$ . We analyzed data in the 3D limit previously<sup>21</sup> according to Eqs. (10) and (12) and found reasonable agreement over a limited temperature range (96.7–101.5 K) just above  $T_c$ . We found that the fluctuation Hall conductivity was positive and the value of  $\alpha$  coming of the analysis ( $-0.04$ ) was small, indicating that the MT process dominates the AL process. In the present paper we extend the analysis to cover the entire temperature range (96.7–178 K) by comparing to layered-structure forms for  $\Delta\sigma_{mm}$  and  $\Delta\sigma_{ab}$ . The form of the layered-structure AL term of  $\Delta\sigma_{mm}$  was calculated by Lawrence and Doniach<sup>22</sup> (LD) as

$$\Delta\sigma_{mm}^{LD} = \frac{e^2}{16\hbar s} f^{LD}(\eta), \quad (14)$$

where

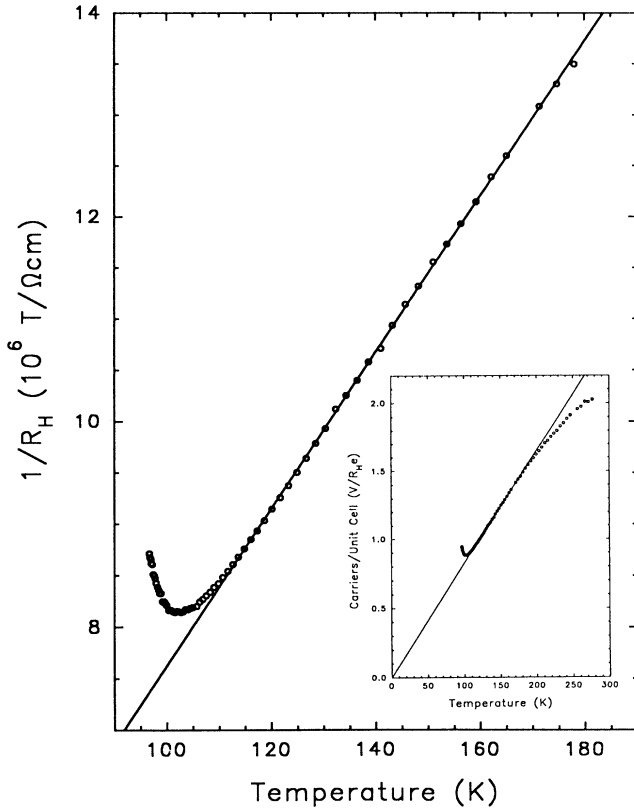


FIG. 4. Reciprocal of the Hall coefficient  $R_H$ . The line is a fit of a range of the data to Eq. (7), giving  $c = 7.624 \times 10^4$  T/( $\Omega$  cm K). Inset: The carrier concentration determined from the Hall coefficient. Here  $V$  is the unit-cell volume. The line is the same fit as above.

$$f^{\text{LD}}(\eta) = \eta^{-1} \left[ 1 + \frac{1}{d^2 \eta} \right]^{-1/2}. \quad (15)$$

The form of the layered-structure MT term of  $\Delta\sigma_{mm}$  was recently calculated by Maki and Thompson<sup>15</sup> and independently by Hikami and Larkin<sup>16</sup> as

$$\Delta\sigma_{mm}^{\text{MT}} = \frac{e^2}{16\hbar s} 4f^{\text{MT}}(\eta), \quad (16)$$

where

$$f^{\text{MT}}(\eta) = \frac{1}{\eta - \delta} \ln \left[ \frac{\eta^{1/2} + \eta^{1/2}(1 + 1/d^2\eta)^{1/2}}{\delta^{1/2} + \delta^{1/2}(1 + 1/d^2\delta)^{1/2}} \right]. \quad (17)$$

The total fluctuation conductivity is thus

$$\Delta\sigma_{mm} = \frac{e^2}{16\hbar s} [4f^{\text{MT}}(\eta) + f^{\text{LD}}(\eta)]. \quad (18)$$

Equation (18) reduces to Eqs. (10a) and (10b) in the 3D and 2D limits if, in the 3D limit, one also assumes that  $\delta \ll \eta$ .

We now turn to  $\Delta\sigma_{ab}$ . Ullah and Dorsey<sup>23</sup> (UD) have recently calculated the temperature dependence of the AL term of  $\Delta\sigma_{ab}$  for the layered-structure model. In the low-field limit [ $H/H_{c2}(0) \ll \eta$ ], they find

$$f^{\text{UD}}(\eta) = \frac{1 + 3d^2\eta + 2d^4\eta^2}{\eta^{3/2}(1 + d^2\eta)^{5/2}}. \quad (19)$$

Supplying the needed coefficient to obtain the temperature dependence of the AL term in  $\Delta\sigma_{ab}$ , we see that

$$\Delta\sigma_{ab}^{\text{UD}} = \frac{e^2}{16\hbar\xi_c(0)} \left[ \frac{7\pi\alpha}{36} \right] \frac{\sigma_{ab}^0}{\sigma_{mm}^0} f^{\text{UD}}(\eta). \quad (20)$$

(see *Note added in proof*). We know of no theoretical calculation giving the temperature dependence of the MT term of  $\Delta\sigma_{ab}$  for a layered structure. However, by comparison of Eqs. (10) and (12) we see that the MT terms of  $\Delta\sigma_{mm}$  and  $\Delta\sigma_{ab}$  have the same dependence on  $\eta$  and  $\delta$  in both the 2D and 3D limits. Based on this, we assume that the  $\eta$  and  $\delta$  dependences of the MT term of  $\Delta\sigma_{ab}$  in the layered-structure model are the same as those of  $\Delta\sigma_{mm}$ , namely,  $f^{\text{MT}}(\eta)$ . With this ansatz the form for the fluctuation Hall conductivity in the layered-structure model is

$$\Delta\sigma_{ab} = \frac{e^2}{8\hbar s} \frac{\sigma_{ab}^0}{\sigma_{mm}^0} \left[ 4f^{\text{MT}}(\eta) + \frac{7\pi}{36} \alpha d f^{\text{UD}}(\eta) \right]. \quad (21)$$

The coefficients of the MT and AL terms here were chosen so that Eq. (21) reduces to Eq. (12a) in the 3D limit. The MT term reduces to that of Eq. (12b) in the 2D limit, but the AL terms of Eqs. (21) and (12b) disagree in the 2D limit by a factor of 14. This discrepancy between the UD form and the form of Fukuyama, Ebisawa, and Tsuzuki may be important from a theoretical point of view, but as we will see below, the MT term dominates the AL term when Eq. (21) is fitted to the Hall conductivity data, since  $\alpha$  turns out to be near zero. Also, the data do not extend fully into the 2D regime. These two factors have the effect of reducing the overall theoretical

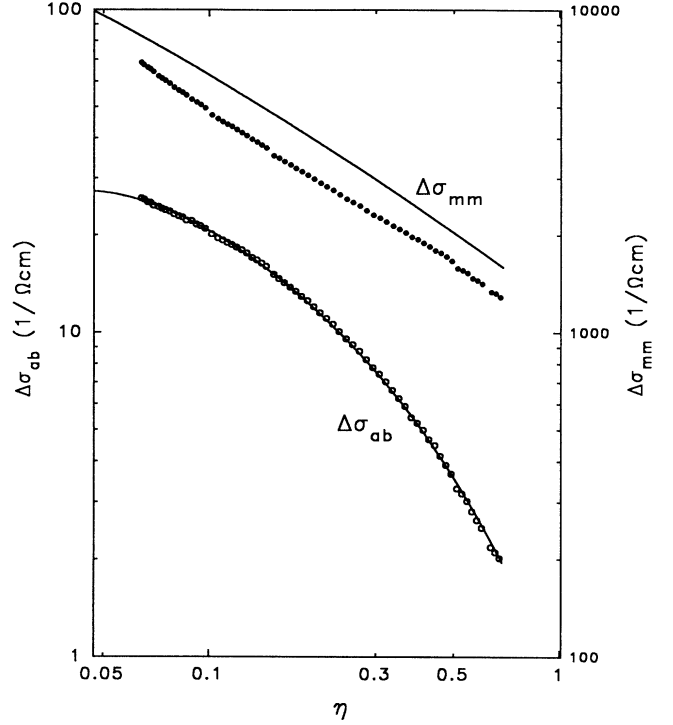


FIG. 5. Fluctuation contribution to the conductivity and Hall conductivity as a function of reduced temperature  $\eta = \ln(T/T_c)$  with theoretical curves determined by fitting to the Hall conductivity.

discrepancy in  $\Delta\sigma_{ab}$  to less than 2% on the high-temperature end of the scale. On the low-temperature end, the AL term has a stronger divergence than the MT term as  $T_c$  is approached, and so the overall theoretical discrepancy rises to about 10%.

We compared the data to the predicted forms for both the conductivity and Hall conductivity. The conductivity  $\sigma_{mm}$  is described by Eq. (4) using Eq. (6) for  $\sigma_{mm}^0$  and Eq. (18) for  $\Delta\sigma_{mm}$ . The Hall conductivity  $\sigma_{ab}$  is described by Eq. (5) using Eq. (8) for  $\sigma_{ab}^0$  and Eq. (21) for  $\Delta\sigma_{ab}$ . There are seven adjustable parameters:  $a$ ,  $b$ ,  $T_c$ ,  $s$ ,  $\xi_c(0)$ ,  $\delta$ , and  $\alpha$ . We first fit the Hall conductivity by varying all seven parameters, using a Levenberg-Marquardt-based nonlinear least-squares fitting routine.<sup>24</sup> We then performed the fit again, using a simulated-annealing fitting routine.<sup>25</sup> Both routines gave the same results, suggesting that the resulting parameters provide the best global fit in our parameter space. We obtained an excellent fit to the Hall conductivity data, as shown in Fig. 5. These same parameters were used to calculate the conductivity, which is also shown in Fig. 5. For this procedure, the Hall conductivity is fit much better than the conductivity. The resulting parameters are listed in Table I (see *Note added in proof*).

We then tried the opposite procedure: We fit the conductivity by varying the parameters and obtained the fit shown in Fig. 6. Again, both routines gave the same fit. The same parameters were then used to calculate the Hall

TABLE I. Values of parameters giving the fits in Figs. 5–7.

	$a$ ( $\mu\Omega$ cm/K)	$b$ ( $\mu\Omega$ cm)	$T_c$ (K)	$s$ ( $\text{\AA}$ )	$\xi_c(0)$ ( $\text{\AA}$ )	$\delta$	$\alpha$
Figure 5	0.4645	2.072	90.69	11.80	1.30	0.0013	-0.076
Figure 6	0.4696	1.100	94.35	9.50	2.40	0.0101	0.017
Figure 7	0.4607	1.546	89.21	11.86	1.67	0.0103	0.081

conductivity which is also shown in Fig. 6. For this procedure the conductivity is fit much better than the Hall conductivity, and the parameters used are again shown in Table I.

We then tried a third procedure: We fit both the conductivity and Hall conductivity simultaneously, in an attempt to get equally good fits for both quantities. To achieve the simultaneous fit, we used a version of the simulated annealing algorithm in which steps were taken in parameter space only if they gave a better fit for both  $\Delta\sigma_{ab}$  and  $\Delta\sigma_{mm}$ . This fit is shown in Fig. 7, and the parameters are listed in Table I.

Referring to Table I, we see that the fits yield physically reasonable values for the adjustable parameters. In agreement with the results of other investigators,<sup>5,26</sup> we find that the zero-temperature Ginzburg-Landau coherence length along the  $c$  axis is about 1.5  $\text{\AA}$ . The layer spacing  $s$  is near to that of the  $c$ -axis lattice parameter 11.68  $\text{\AA}$ . This indicates that the two copper-oxide planes in  $\text{YBa}_2\text{Cu}_3\text{O}_{7-x}$ , which are spaced by 3.2  $\text{\AA}$ , are tightly

coupled, acting as one superconducting layer. This is in contrast to an earlier result of Friedmann *et al.*,<sup>2</sup> where lower values of  $s$  and  $\xi_c(0)$  were found, presumably because Friedmann *et al.* used a layered-structure model which only included the AL term, ignoring the MT term.

From the MT pair-breaking parameter  $\delta$ , we calculate the phase-relaxation time  $\tau_\phi$  according to

$$\tau_\phi = \frac{\pi\hbar}{8k_B T\delta}. \quad (22)$$

The values at  $T=100$  K from each of our fits are on the order of a few picoseconds, which is 10–100 times longer than that of 0.1 ps from Ref. 5 or 26. This might reflect the fact that the resistivity of our sample is lower than the samples used in those studies.

In Fig. 8 we show the  $\Delta\sigma_{ab}$  fit of Fig. 5 on a semilogarithmic plot to display the relative proportions of the MT and AL terms. The AL term gives a negative contribution for this fit, since  $\alpha$  is negative. Note the dominance of the MT term, especially on the high-temperature end of the scale. In Fig. 9 we plot the  $\Delta\sigma_{mm}$  fit of Fig. 6 on a semilogarithmic plot, again showing the relative propor-

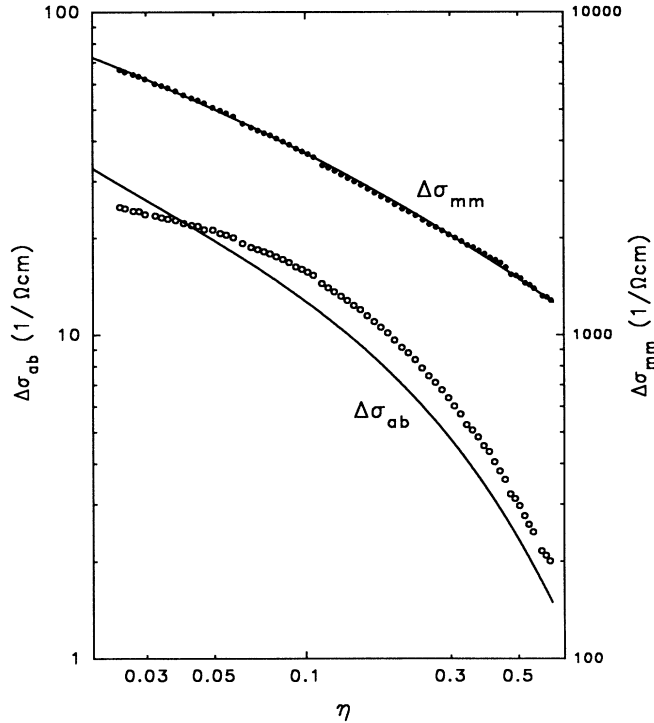


FIG. 6. Fluctuation contribution to the conductivity and Hall conductivity as a function of  $\eta$ , with theoretical curves determined by fitting to the conductivity.

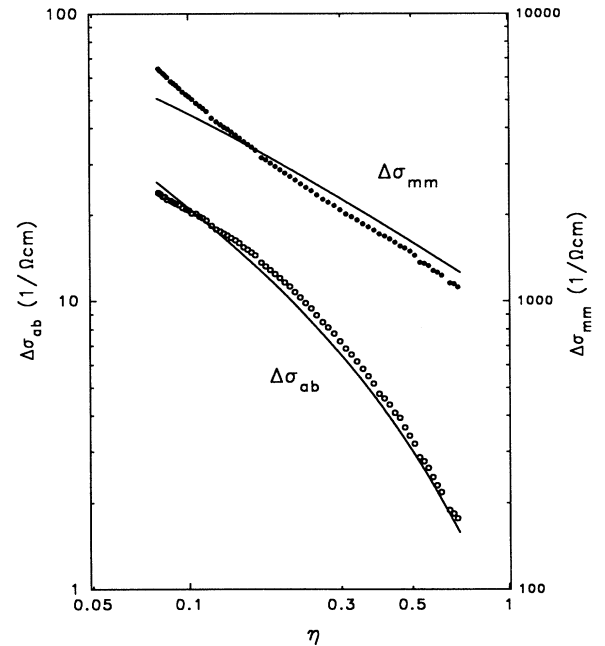


FIG. 7. Fluctuation contribution of the conductivity and Hall conductivity as a function of  $\eta$ , with theoretical curves determined by simultaneously fitting to both data sets.

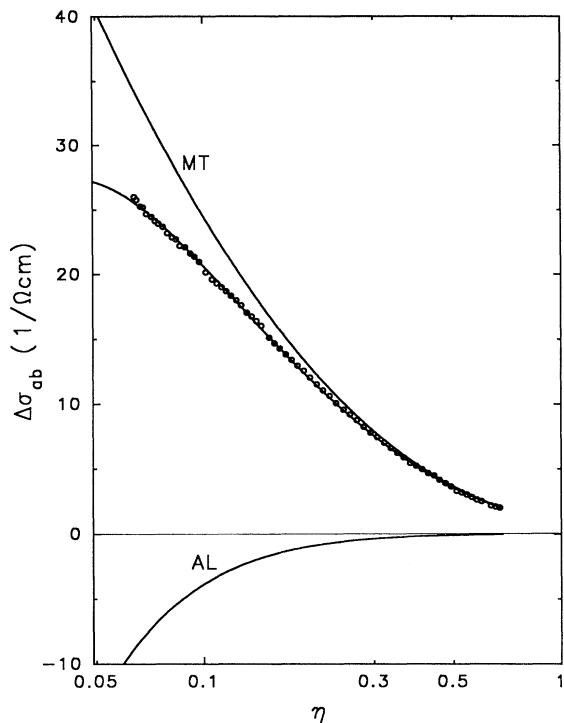


FIG. 8. Semilogarithmic plot of the fluctuation *Hall conductivity* of Fig. 5, showing the relative proportions of the two terms, labeled as MT and AL.

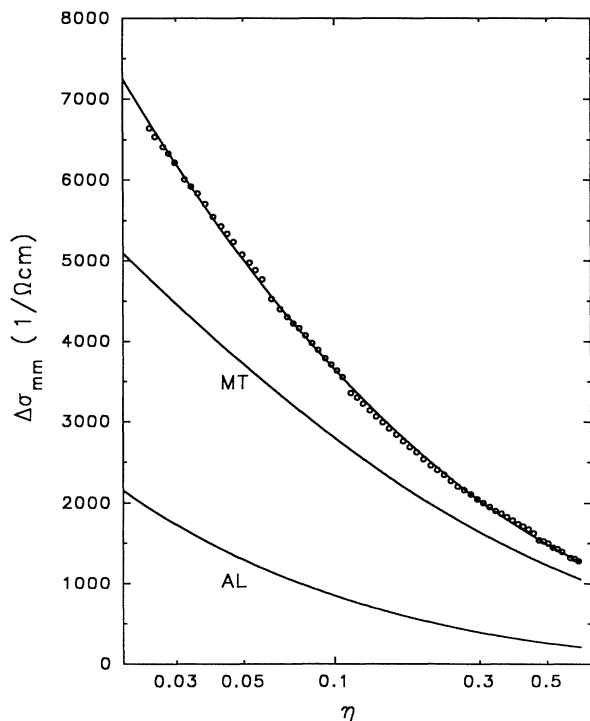


FIG. 9. Semilogarithmic plot of the fluctuation *conductivity* of Fig. 6, showing the relative proportions of the two terms, labeled as MT and AL.

tions of the MT and AL terms.

In Fig. 10 we plot the cotangent of the Hall angle versus  $T^2$ . This shows that the tangent of the Hall angle,  $\rho_{ab}/\rho_{bb}$ , varies approximately as  $1/T^2$  in the normal state, which is consistent with the observation that the resistivity and  $1/R_H$  are approximately proportional to  $T$ . The inset of Fig. 10 shows the fluctuation-induced deviation away from this behavior just above  $T_c$ .

## VI. CONCLUSIONS

We have presented Hall-effect data and resistivity data measured on an untwinned single crystal of  $\text{YBa}_2\text{Cu}_3\text{O}_{7-x}$ . The normal-state in-plane resistivity is linear in temperature with a small, positive, zero-temperature intercept  $b$ . The reciprocal of the normal-state Hall coefficient is linear in temperature with a zero intercept. The deviations from linearity just above  $T_c$  can be interpreted within a model of thermodynamic fluctuations in a layered superconductor. Introducing an ansatz, we have extended this layered-structure model to include the effect of the Maki-Thompson process on the fluctuation Hall conductivity. We obtain fairly good fits of this model to our data, with physically reasonable pa-

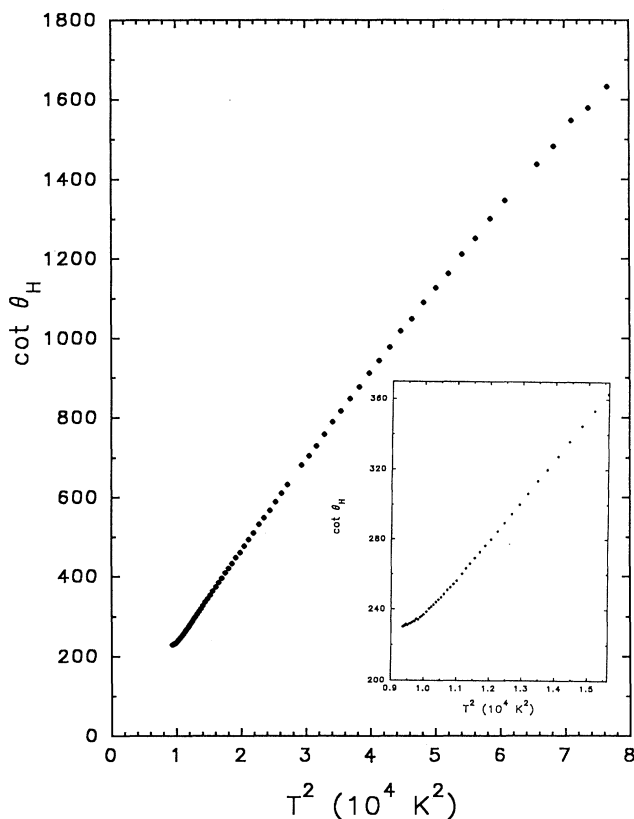


FIG. 10. The cotangent of the Hall angle plotted as a function of  $T^2$ . These data are for  $H$  along  $c$ ,  $J$  along  $b$ . Inset: Expanded view of the region just above  $T_c$ , showing the effect of fluctuations.

rameters. The fits could be better, indicating that the model does not include all of the significant features of the system.

The fits to our data yield values of  $\xi_c(0)$  between 1.3 and 2.4 Å, indicating that  $\text{YBa}_2\text{Cu}_3\text{O}_{7-x}$  behaves in a nearly two-dimensional way, except near  $T_c$ . The value of  $s$ , the distance between superconducting layers, is approximately equal to the  $c$ -axis lattice parameter. This implies that the two copper-oxide planes in the unit cell are tightly coupled, acting as one superconducting layer.

We obtain a value of the phase-relaxation time  $\tau_\phi$  of a few picoseconds, and as a result, the Hall-effect fluctuations are dominated by the Maki-Thompson process rather than the Aslamazov-Larkin process. Our data indicate that  $\Delta\sigma_{ab}$  is positive above  $T_c$  in the low-field limit [ $H/H_{c2}(0) \ll \eta$ ], in contrast to the results of Iye, Nakamura, and Tamegai<sup>6</sup> for a twinned thin film of  $\text{ErBa}_2\text{Cu}_3\text{O}_{7-x}$ . Since the MT term can only be positive, Iye, Nakamura, and Tamegai concluded that  $\alpha$  is negative and that its magnitude is large enough so that the AL term dominates, thus giving the negative value that they observed. According to the original theory of Fukuyama, Ebisawa, and Tsuzuki,<sup>19</sup>  $\alpha$  is proportional to the energy derivative of the density of states at the Fermi level and can be either positive or negative, depending upon the material. The microscopic interpretation of  $\alpha$  within the layered-structure model used here is not as clear. We conclude, however, that  $\alpha$  has a small magnitude, and so the Maki-Thompson process dominates the fluctuation Hall conductivity for untwinned  $\text{YBa}_2\text{Cu}_3\text{O}_{7-x}$ .

The parameter  $\alpha$  is proportional to the particle-hole asymmetry parameter  $\lambda_0^{-1}$  discussed by Ullah and Dorsey.<sup>23</sup> This parameter must be nonzero for the Hall effect even to exist in a material, and the fact that it turns out to be small in our experiment makes one suspicious that

there might be a certain degree of symmetry between electrons and holes in  $\text{YBa}_2\text{Cu}_3\text{O}_{7-x}$ . It is interesting that the  $1/T$  dependence of  $R_H$  in this material can also be explained if one assumes a certain degree of symmetry between electrons and holes.<sup>27</sup>

*Note added in proof.* In a private communication, A. T. Dorsey has alerted us to problems with some of the theoretical papers. In Eq. (4.2) of Ullah and Dorsey (Ref. 23), the denominator appearing in square brackets should be raised to the  $\frac{1}{2}$  power. This does not affect our discussion or conclusions, however. Of greater importance for us is that, also in Ref. 23, the right-hand side of Eq. (4.13) needs to be divided by  $2\phi_0$ . It then agrees in the 2D limit with Eq. (2.33) of Ref. 19, but a disagreement remains in the 3D limit between the theory of Refs. 19 and 23, which Dorsey has traced to the derivation of Eq. (2.32) in Ref. 19. When this is corrected, one finds a result that agrees with Ref. 23. As a result of these corrections,  $\alpha$  in our Eqs. (12a), (20), and (21) should be replaced by  $\alpha/14$ . This removes the discrepancy that we remarked on following Eq. (21), and *the values of  $\alpha$  listed by us in Table I must all be multiplied by 14*. In another recent calculation, Dorsey has verified our ansatz that the  $\eta$  and  $\delta$  dependences of the MT term in  $\Delta\sigma_{ab}$  in the layered-structure model are the same as those of the MT term in  $\Delta\sigma_{mm}$ .

#### ACKNOWLEDGMENTS

We thank T. A. Friedmann, S. E. Stupp, R. L. Dudev, W. C. Lee, and V. Kalmeyer for helpful discussions regarding this work. This research was supported in part by National Science Foundation Grant No. DMR 90-17371 (J.P.R. and D.M.G.) and in part by the National Science Foundation (DMR 88-09854) through the Science and Technology Center for Superconductivity (J.G.).

- <sup>1</sup>P. P. Freitas, C. C. Tsuei, and T. S. Plaskett, Phys. Rev. B **36**, 833 (1987).
- <sup>2</sup>T. A. Friedmann, J. P. Rice, J. Giapintzakis, and D. M. Ginsberg, Phys. Rev. B **39**, 4258 (1989).
- <sup>3</sup>S. E. Inderhees, M. B. Salamon, J. P. Rice, and D. M. Ginsberg, Phys. Rev. Lett. **66**, 232 (1991).
- <sup>4</sup>W. C. Lee, R. A. Klemm, and D. C. Johnston, Phys. Rev. Lett. **63**, 1012 (1989).
- <sup>5</sup>Y. Matsuda, T. Hirai, S. Komiyama, T. Terashima, Y. Bando, K. Iijima, K. Yamamoto, and K. Hirata, Phys. Rev. B **40**, 5176 (1989).
- <sup>6</sup>Y. Iye, S. Nakamura, and T. Tamegai, Physica C **159**, 616 (1989).
- <sup>7</sup>S. L. Cooper, F. Slakey, M. V. Klein, J. P. Rice, E. D. Bukowski, and D. M. Ginsberg, Phys. Rev. B **38**, 11934 (1988).
- <sup>8</sup>D. E. Farrell, J. P. Rice, and D. M. Ginsberg, Phys. Rev. Lett. **67**, 1165 (1991).
- <sup>9</sup>T. A. Friedmann, M. W. Rabin, J. Giapintzakis, J. P. Rice, and D. M. Ginsberg, Phys. Rev. B **42**, 6217 (1990).
- <sup>10</sup>J. P. Rice, and D. M. Ginsberg, J. Cryst. Growth **109**, 432 (1991).

- <sup>11</sup>I. Isenberg, B. R. Russell, and R. F. Greene, Rev. Sci. Instrum. **19**, 685 (1948).
- <sup>12</sup>T. Penney, S. von Molnar, D. Kaiser, F. Holtzberg, and A. W. Kleinsasser, Phys. Rev. B **38**, 2918 (1988).
- <sup>13</sup>J. Clayhold, S. Hagen, Z. Z. Wang, N. P. Ong, J. M. Tarascon, and P. Barboux, Phys. Rev. B **39**, 777 (1989).
- <sup>14</sup>L. Onsager, Phys. Rev. **38**, 2265 (1931).
- <sup>15</sup>K. Maki and R. S. Thompson, Phys. Rev. B **39**, 2767 (1989).
- <sup>16</sup>S. Hikami and A. I. Larkin, Mod. Phys. Lett. B **2**, 693 (1988).  
Note that the  $\delta$  defined by Hikami and Larkin is *not* the Maki-Thompson pair-breaking parameter  $\delta$ , although the two parameters are related to each other by  $\delta_{\text{HL}} = 1/2d^2\delta$ , where  $\delta_{\text{HL}}$  denotes the  $\delta$  defined by Hikami and Larkin and  $d$  is defined in our Eq. (13). This Hikami-Larkin notation was also used in Refs. 5 and 26.
- <sup>17</sup>L. G. Aslamazov and A. I. Larkin, Fiz. Tverd. Tela (Leningrad) **10**, 1104 (1968) [Sov. Phys. Solid State **10**, 875 (1968)].
- <sup>18</sup>K. Maki, Prog. Theor. Phys. (Kyoto) **39**, 897 (1968); R. S. Thompson, Phys. Rev. B **1**, 327 (1970).
- <sup>19</sup>H. Fukuyama, H. Ebisawa, and T. Tsuzuki, Prog. Theor. Phys. **46**, 1028 (1971).
- <sup>20</sup>For comparison of Eqs. (10) and (12) to Eqs. (2.32)–(2.35) of

Ref. 19, we observe that

$$\frac{e^2}{32\hbar\xi(0)} = \frac{3}{16} \left[ \frac{3k_B T_c}{\epsilon_F} \right]^{1/2} \left[ \frac{\pi\hbar}{p_F l} \right]^{3/2} \frac{ne^2\tau}{m},$$

which is valid in the weak-coupling dirty limit. Note that Eq. (2.34) of Ref. 19 only quotes the AL term of  $\Delta\sigma_{mm}^{(3D)}$ . In Eq. (10a) we have added the 3D MT term with the same  $T$  dependence and with a coefficient 4 times that of the AL term, as required by Eqs. (1) and (4) of Ref. 15.

<sup>21</sup>D. M. Ginsberg, J. P. Rice, T. A. Friedmann, and J. M. Mochel (unpublished).

<sup>22</sup>W. E. Lawrence and S. Doniach, in *Proceedings of the Twelfth*

*International Conference on Low Temperature Physics*, Kyoto, 1970, edited by Eizo Kanda (Keigaku, Tokyo, 1971), p. 361.

<sup>23</sup>S. Ullah and A. T. Dorsey, *Phys. Rev. B* **44**, 262 (1991).

<sup>24</sup>W. H. Press, B. P. Flannery, S. A. Teukolsky, and W. T. Vetterling, *Numerical Recipes* (Cambridge University Press, Cambridge, England, 1986), p. 523.

<sup>25</sup>A. Corana, M. Marchesi, C. Martini, and S. Ridella, *ACM Trans. Math. Software* **13**, 262 (1987).

<sup>26</sup>K. Winzer and G. Kumm, *Z. Phys. B* **82**, 317 (1991). Note that Eq. (3) of this reference, which quotes Eq. (3.9) of Hikami and Larkin (Ref. 16), has a typographic error: the 2 in the denominator of the logarithm should be a 1.

<sup>27</sup>A. Davidson, P. Santhanam, A. Palevski, and M. J. Brady, *Phys. Rev. B* **38**, 2828 (1988).